The Egyptian Journal of Radiology and Nuclear Medicine (2014) **45**, 443–453

Egyptian Society of Radiology and Nuclear Medicine

The Egyptian Journal of Radiology and Nuclear Medicine

www.elsevier.com/locate/ejrnm
www.sciencedirect.com

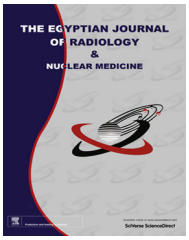

ORIGINAL ARTICLE

Can unenhanced multiparametric MRI substitute gadolinium-enhanced MRI in the characterization of vertebral marrow infiltrative lesions?

Dalia Z. Zidan [a,*], **Hesham A. Elghazaly** [b]

[a] *Department of Radiodiagnosis, Ain Shams University, Cairo, Egypt*
[b] *Department of Clinical Oncology, Ain Shams University, Cairo, Egypt*

Received 19 November 2013; accepted 21 February 2014
Available online 20 March 2014

KEYWORDS

Multiparametric MRI;
Gadolinium enhanced MRI;
Diffusion weighted imaging;
Apparent diffusion coefficient;
Chemical shift imaging

Abstract *Purpose:* To assess the diagnostic effectiveness of unenhanced-multiparametric magnetic resonance imaging (mp MRI) as an alternative to gadolinium (Gad)-enhanced MRI in the characterization of vertebral marrow infiltrative lesions.
Patients and methods: A prospective evaluation of fifty-six patients with suspected or untreated vertebral metastases undergoing MRI of the spine at 1.5 T was carried out. Two groups of sequences were assigned and compared for the characterization of marrow infiltrative lesions: group [A] unenhanced-mp MRI (including T1-weighted, T2-weighted, short time inversion recovery (STIR), diffusion weighted imaging (DWI) and in/opposed phase sequences) and group [B] gadolinium-enhanced MRI (including T1-weighted, T2-weighted, STIR and T1-weighted fat-suppressed gadolinium-enhanced sequence). Qualitative and quantitative image analysis was performed and compared. The sensitivity, specificity, positive predictive value (PPV), negative predictive value (NPV) and accuracy for both imaging techniques were calculated.
Results: There was no statistical significant difference between unenhanced-multiparametric MRI and gadolinium-enhanced MRI as regards their diagnostic performance in differentiating benign from malignant vertebral marrow infiltrative lesions ($p > 0.05$) with calculated sensitivity (94% vs. 97%), specificity (92% vs. 88%), positive predictive value (94% vs. 91%), negative predictive value (92% vs. 95%) and (93% vs. 93%) accuracy.

* Corresponding author. Tel.: +20 1001155301.
E-mail address: dalia.zidan@yahoo.com (D.Z. Zidan).
Peer review under responsibility of Egyptian Society of Radiology and Nuclear Medicine.

Production and hosting by Elsevier

 http://dx.doi.org/10.1016/j.ejrnm.2014.02.014

Conclusion: Unenhanced-multiparametric MRI is compatible with gadolinium-enhanced MRI in reliable characterization of marrow infiltrative lesions. The routine MRI protocol of cancer patients should be altered to accommodate the evolving MRI technology and cost effectively substitute the need for a gadolinium enhanced scan.

1. Introduction

The vertebral column is the most common site of skeletal metastasis (1). Radionuclide bone scanning has been repeatedly shown to be sensitive but nonspecific (2). Distinguishing normal spinal marrow from pathology is essential to avoid missing pathology or misinterpreting normal changes, either of which may result in unnecessary additional imaging tests (3). MRI is the only imaging technique allowing the direct visualization of bone marrow and is the most sensitive (4). Although standard MR imaging protocol for bone marrow with T1-weighted, STIR and T2-weighted techniques is very sensitive, findings on images are not specific (5). Recent developments in advanced MR techniques and postprocessing software have expanded the use of MR imaging to include quantitative analysis (6).These advances allow for the objective analysis of composition (7) and architecture down to a molecular level (8,9). New techniques were tried for distinguishing between malignant and benign bone marrow with varying success. These included chemical shift imaging (10,11) and diffusion-weighted MR imaging allowing for increased conspicuity of lesions (12). In equivocal findings of bone marrow lesions gadolinium enhanced study may be done. Although this increases the length and expense of the MR examination, it is not clear if it improves diagnosis (13).

Thus, the purpose of this study was to assess the diagnostic effectiveness of unenhanced multiparametric magnetic resonance imaging (mp MRI) as an alternative to gadolinium-enhanced MRI in the characterization of vertebral marrow infiltrative lesions.

2. Patients and methods

2.1. Patients

This prospective study included a total of 56 patients, who were examined between January 2012 and June 2013, at the Ain Shams University Hospital MRI Unit. All patients included in this study were referred from the clinical oncology department at the Ain Shams University Hospital with a history of known primary malignancy and clinically suspected or untreated vertebral metastases. Patients with multifocal or diffuse disease pattern were included and patients with solitary focal vertebral marrow lesion or treated marrow deposits were excluded from the study group. Other exclusion criteria were pregnancy, contraindications to MRI (e.g., cardiac pacemaker) and severe renal insufficiency with glomerular filtration rate <30 ml/min and serum creatinine >2.0 mg/dl.

The study group consisted of 31 male and 25 female patients, with a mean age of 46 years (age range, 4–83 years). The known primary tumors of the 56 patients were lymphoma ($n = 18$), carcinoma of breast ($n = 11$), leukemia (10), multiple myeloma ($n = 8$), carcinoma of prostate ($n = 5$) and bronchogenic carcinoma ($n = 4$).

All patients had provided written consent for the MRI studies.

2.2. MRI technique

MR imaging of the spine of the 56 patients included examination of the cervical ($n = 7$), dorsal ($n = 18$) and lumbosacral ($n = 39$) regions, as 2 patients had undergone cervicodorsal study, 4 patients dorsolumbar study and one patient whole spine study.

All examinations were performed on a 1.5 MR scanner (Achieva; Philips Medical Systems, Bothell, WA, USA) using a spine radio-frequency surface array coil. All Patients had a history of known primary malignancy, therefore they received gadolinium as part of the routine protocol of cancer patient at our MRI unit which consists of the following sequences:

Unenhanced sagittal and axial T1-weighted fast spin-echo sequence, a sagittal and axial T2-weighted fast spin-echo sequence, a sagittal T2-weighted STIR sequence and a contrast-enhanced sagittal and axial T1-weighted sequence with fat suppression. In this study sagittal diffusion-weighted imaging and chemical shift (in/opposed phase) sequences were added to the protocol. The scan parameters were set as follows:

Sagittal T1-weighted turbo spin echo images were acquired (TR/TE, 424/9; number of slices, 12; slice thickness, 4 mm; gap, 0.4 mm; flip angle, 80°; FOV, 300 mm^2). The total imaging time was 1:54 min.

Axial T1-weighted turbo spin echo images were done(TR/TE, 575/10; number of slices, 25; slice thickness, 5 mm; gap, 0.5 mm; flip angle, 90°; FOV, 200 mm^2). The total scan duration was 1:46 min.

Sagittal T2-weighted turbo spin echo images were performed (TR/TE, 2578/100; number of slices, 12; slice thickness, 4 mm; gap, 0.4 mm; flip angle, 90°; FOV, 300 mm^2). The total imaging time was 1:51 min.

Axial T2-weighted turbo spin echo images were performed(TR/TE, 3000/100; number of slices, 25; slice thickness, 5 mm; gap, 0.5 mm; flip angle, 90°; FOV, 200 mm^2). The total imaging time was 1:06 min.

Sagittal T2-weighted STIR images were acquired (TR/TE, 3761/80; number of slices, 12; slice thickness, 3.8 mm; gap, 1.2 mm; flip angle, 90°; FOV, 300 mm^2). The total imaging duration was 2:08 min.

In addition to the routine sequences, sagittal in-phase (TR/TE, 10/4.6; number of slices, 12; slice thickness, 4 mm; gap, 1 mm; flip angle, 15°; FOV, 300 mm^2 and the total imaging duration was 14.1 s) and opposed-phase gradient recalled-echo sequences (TR/TE, 10/2. 3; number of slices, 12; slice thickness, 4 mm; gap, 1 mm; flip angle, 15°; FOV, 300 mm^2 and the total imaging duration was 13.6 s) were acquired.

DWI was performed with free breathing and inversion recovery single-shot spin-echo echo-planar sequences (TR/TE, 9000/68; number of slices, 12; slice thickness, 5 mm; gap, 0 mm; flip angle, 90°; FOV, 300 mm^2).

We applied 3 diffusion-sensitizing gradients with *b*-values of 0, 50 and 800 s/mm^2. The total imaging time was 6:09 min.

After manual intravenous administration of 0.1 mmol/kg of gadolinium-DTPA, axial and sagittal T1-weighted fat suppressed sequences with the following parameters were applied: TR/TE, 574/10; number of slices, 12; slice thickness, 4 mm; gap, 0 mm; flip angle, 90°; FOV, 300 mm^2). The total scan duration was 1:43 min for sagittal images and 2:26 min for axial scan.

2.3. Image analysis

All images were loaded to a workstation (HPZR 24 W; Philips Medical Systems). Bone marrow evaluation and image interpretation were performed by two radiologists with expertise in musculoskeletal MRI working in consensus. During the MR image analysis, the radiologists were blinded to the clinical history or previous radiologic reports of the study patients. The images of the applied sequences were divided into two groups and the radiologists interpreted each group separately. The first group (A) included the unenhanced mp MRI sequences (T1-weighted, T2-weighted, STIR, DWI and in/opposed phase imaging) and the second group (B) consisted of gadolinium-enhanced T1-weighted fat-suppressed sequence in addition to the conventional T1-weighted, T2-weighted and STIR sequences.

2.3.1. Qualitative analysis

Bone marrow signal intensity was qualitatively analyzed by visually comparing its signal intensity with the signal intensity of the non-degenerated intervertebral disc, subcutaneous fat and muscle tissue depicted on T1-weighted images.

For MRI interpretation, we used previously established diagnostic criteria for vertebral bone marrow evaluation to include: Malignant marrow lesions, whether multifocal or diffuse, were defined as those being isointense or hypointense to muscle or intervertebral disc on T1-weighted images with corresponding hyperintensity on T2-weighted or STIR images (14–16), hyperintense on the DWI with a high *b*-value (*b*-value = 800), lack normal signal dropout on out-of-phase compared with in-phase images (17) and show avid post contrast enhancement (3).

On the other hand bone marrow lesion with signal intensity on T1-weighted images higher than disk and muscle, with no abnormal signal changes on STIR images (18), with a signal dropout on out-of-phase imaging compared with in-phase images (17), not hyperintense on high b value DWI and did not show post contrast enhancement (14) was defined as benign.

2.3.2. Quantitative analysis

Image post-processing was performed using a workstation (HP ZR 24 W; Philips Medical Systems). The radiologist quantitatively evaluated the bone marrow signal intensity by performing measurements in regions of interest (ROI). Hyperintense lesions on the DWI with a high *b*-value (*b* 800) which correspond to signal intensity changes on the T1-weighted spin-echo MR images were identified and the regions of interest were manually drawn trying to stay within the confines of the hyperintensity.

The ROI was lesion-size-dependent in localized discrete lesions, but in diffuse vertebral marrow lesions it was drawn as large as possible placed in the antrocentral aspect of vertebral body to avoid vertebral end plate degenerative changes and basivertebral vein plexus. The regions of interest varied between 5 and 15 mm in diameter. In each patient at least 3 ROI were applied. The ROIs were copied into the computer memory and pasted onto registered ADC maps.

ADC values were automatically calculated using the software provided by the MR scanner manufacturer (Diffusion Calculation: Philips Medical Systems) and the ADC quantitative parameter was expressed in square millimeters per second as mean ± SD. The average ADC value of the three regions of interest of each patient was calculated and recorded.

The final diagnosis which was made on the basis of biopsy results or results of clinical and radiologic follow-up for at least 6 months, was used as the ''gold standard'' to classify the vertebral marrow infiltrative lesions as benign or malignant.

2.4. Statistical analysis

The one-way analysis of variance (ANOVA) test was used for comparison between 5 independent mean groups for parametric data to determine the significance between the ADC values of the malignant, normal, inflammatory, osteoporotic and red marrow lesions.

All values were expressed as mean ± SD for quantitative ADC parametric measures. If the probability of error (*p*-value) is less than 0.05, the result was considered statistically significant, while at 0.01 and 0.001 was highly and extremely significant, respectively.

IBM SPSS statistics (V. 21.0, IBM Corp., USA, 2012) and GraphPad Prism 6 for Windows version 6.03(GraphPad Software, San Diego, CA, USA) were used for data analysis. The diagnostic validity test was done for both unenhanced multiparametric magnetic resonance imaging (mp MRI) and gadolinium-enhanced MRI for vertebral marrow infiltrative lesions. It included the diagnostic sensitivity, specificity, positive and negative predictive values and diagnostic accuracy.

3. Results

According to the ''gold standard'' the final results of the 56 patients included in the study were 24 of benign nature and 32 malignant vertebral marrow infiltrative or multifocal lesions. The 24 patients with benign marrow lesions included 7 patients with normal marrow, 9 patients with diffuse yellow to red marrow reconversion due to anemia or induced by bone marrow – stimulating factor and bone marrow transplantation, 5 patients with inflammatory/infectious spondylitis or spondylodiscitis and 3 patients with osteoporosis.

On the other hand the 32 patients with established malignant multifocal or infiltrative vertebral marrow lesions included lymphomatous and leukemic infiltration ($n = 9$ and $n = 7$ respectively), multiple myeloma ($n = 5$) and metastases from breast cancer ($n = 5$), prostate cancer ($n = 4$), and lung cancer ($n = 2$).

According to the criteria of image interpretation previously mentioned in patients and methods using the two groups of sequences (group A) unenhanced-mp MR sequences and (group B) including the conventional sequences and gad-enhanced T1-weighted fat suppressed sequence, lesions were classified as benign and malignant vertebral marrow lesions.

On visual and quantitative assessment of the unenhanced-mp MRI sequences (group A) 22 of 24 patients with proved benign lesions were correctly diagnosed and considered true negative. 8 of the 22 patients with proved benign lesions were initially false interpreted as malignant lesions according to imaging criteria on conventional MRI sequences as they exhibited relatively diffuse homogeneous or heterogeneous decreased marrow signal intensity on the T1-weighted images compared with muscle and non-degenerated intervertebral disc, and increased signal intensity on the T2-weighted and STIR images .4 of these 8 lesions also showed high signal intensity on 800 *b*-value DWI, but their signal dropout on

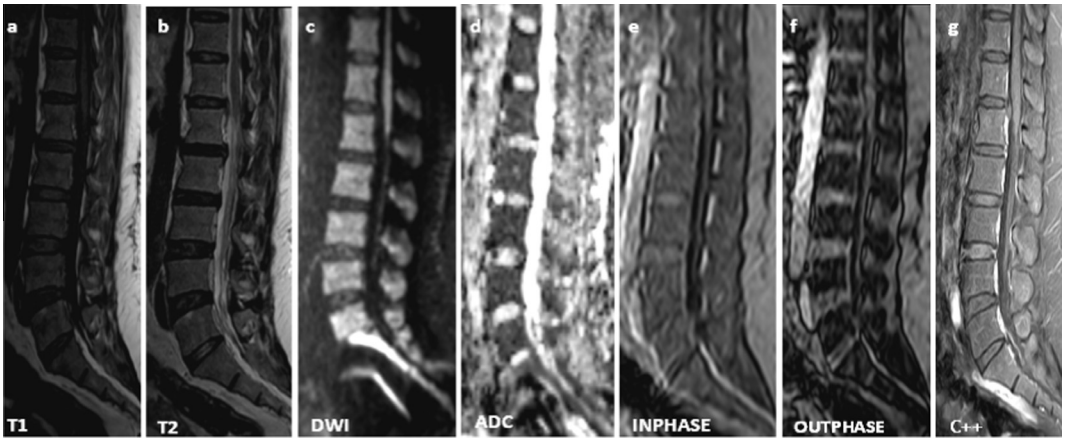

Fig. 1 A 48-year-old female, known case of primary bronchogenic carcinoma, presented with generalized bony aches and fatigue. Unenhanced-mp MRI and gadolinium-enhanced MRI revealed diffuse yellow to red marrow reconversion. (a) Sagittal T1-weighted spin-echo image shows diffuse low signal intensity of lumbosacral vertebrae but still higher than adjacent muscle and isointense to non-degenerated intervertebral disc. (b) Sagittal T2-weighted spin-echo image shows intermediate signal intensity of lumbosacral vertebrae. (c) DW image at *b*-value 800 s/mm^2 shows diffuse hyperintense signal suggesting diffuse marrow infiltration. (d) ADC map shows average apparent diffusion coefficient (ADC) value of 0.402×10^{-3} mm^2/s. (e) In-phase and (f) out-of-phase gradient-echo MR images show normal signal dropout of vertebral marrow on out-of-phase image compared with in-phase (h) confirmed the benign nature of yellow to red marrow reconversion. (g) Sagittal contrast-enhanced T1-weighted fat-suppressed MR image shows mild bone marrow enhancement.

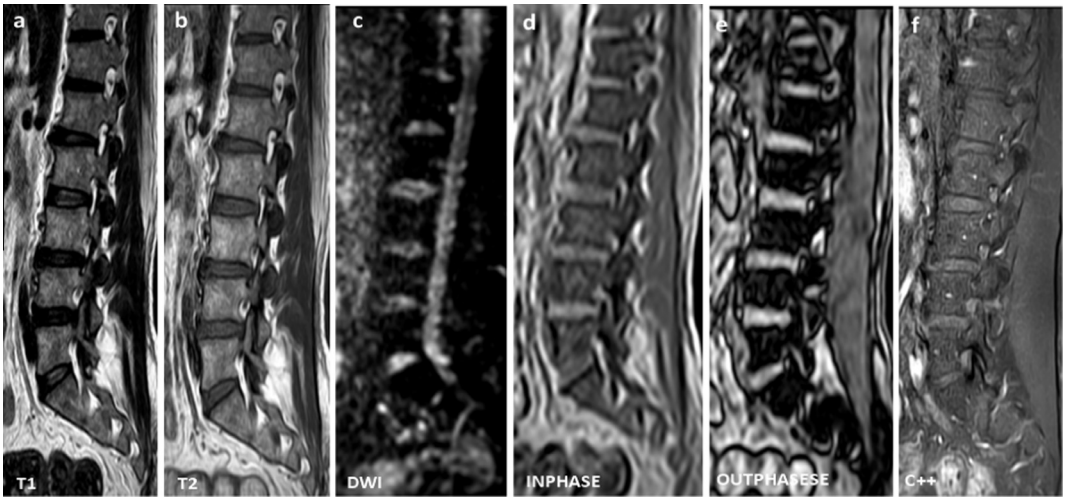

Fig. 2 A 38-year-old man, known case of acute lymphoblastic leukemia, presented with back pain. Unenhanced-mp MRI and gadolinium-enhanced MRI revealed osteoporosis and negative study for bone marrow leukemic infiltration confirmed with a 6 month follow up negative MRI study. (a) Sagittal precontrast T1-weighted spin-echo image and (b) sagittal T2-weighted spin-echo image show diffuse heterogenous signal intensity of lumbosacral vertebrae suspicious of bone marrow infiltration or osteoporotic changes. (c) DW image at *b*-value 800 s/mm^2 shows significantly low marrow signal intensity with average apparent diffusion coefficient (ADC) value of 0.142×10^{-3} mm^2/s. (d) In-phase and (e) out-of-phase gradient-echo MR images show normal signal dropout of vertebral marrow on out-of-phase image compared with in-phase (d). Unenhanced-mp MRI confirmed absence of marrow infiltration. (f) Sagittal gadolinium-enhanced T1-weighted fat-suppressed MR image does not show abnormal enhancement.

opposed phase images confirmed their benign nature of red marrow reconversion (Fig. 1) which was further confirmed on follow up study.

2 of these 8 lesions did not exhibit high signal on 800 *b*-value DWI and exhibition of a signal dropout on opposed phase images also confirmed their benignity and osteoporosis was diagnosed (Fig. 2). On the other hand 2 of the 8 lesions showed diffusion restriction and no signal dropout on opposed phase images, but the measured ADC value was high (average 1.4×10^{-3} mm^2/s), benign inflammatory/infective nature was considered and resolution of abnormal signal intensity on follow up MRI confirmed their benign nature (Fig. 3). 2 of 24 benign lesions were false positive as they met the malignant imaging criteria on all unenhanced-mp MRI included sequences, but histopathological verification and follow up MRI revealed extensive hypercellular hematopoietic marrow after bone marrow transplantation.

Gad-enhanced MRI (group B) correctly diagnosed 21 of 24 proved benign lesions as they did not show postcontrast enhancement apart from three false positive benign lesions that exhibited appreciable contrast enhancement, two of which were diffuse red marrow and the third lesion was spondylitis. Follow up studies with stationary course of the enhancing red marrow and resolution of abnormal signal intensity in spondylitis confirmed their benign nature.

Of the 32 cases with proved malignant lesions, 31 had decreased signal intensity compared with muscle on the T1-weighted images. On the T2-weighted and STIR sequences 5 lesions were isointense to normal marrow; the remaining 26 lesions were hyperintense and metastatic disease was confirmed

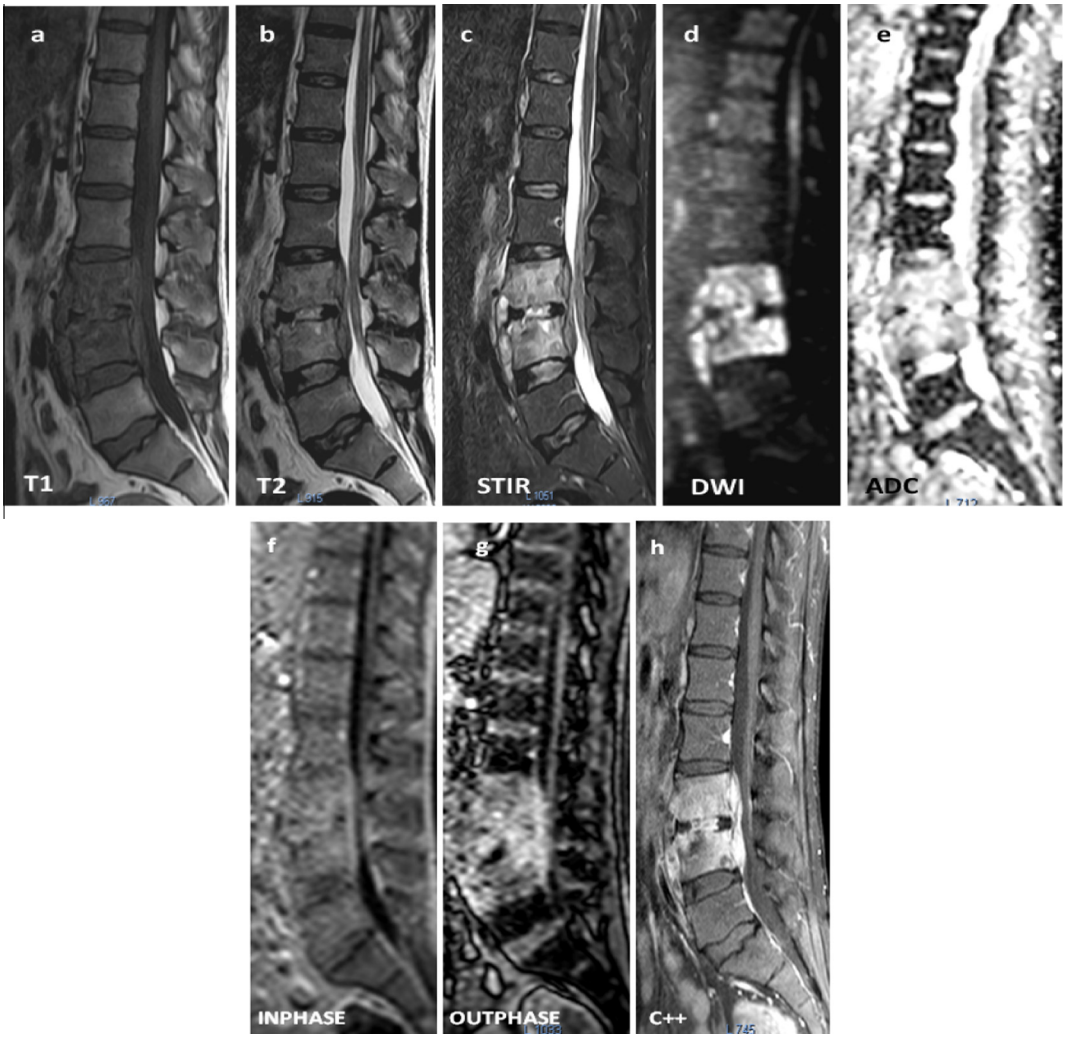

Fig. 3 A 34-year-old man with known bronchogenic carcinoma presented with back pain and fever. Unenhanced-mp MRI and gadolinium-enhanced MRI revealed L3/l4 spondylodiscitis with prevertebral and epidural abscess. (a) Sagittal precontrast T1-weighted spin-echo image shows diffuse low signal intensity of L3 and L4 vertebrae associated with prevertebral and epidural soft tissue mass. (b) Sagittal T2-weighted spin-echo image and sagittal STIR (c) show corresponding high signal intensity and bright signal of L3/4 disc. (d) DWimage at *b*-value 800 s/mm^2 shows diffusion restriction of L3 and L4 vertebrae and intervening disc as well as the prevertebral and epidural component. (e) ADC map shows a high apparent diffusion coefficient (ADC) value of 1.452×10^{-3} mm^2/s, which confirms the inflammatory/infectious nature of the lesion. (f) in-phase and (g) out-of-phase gradient-echo MR images show corresponding brighter signal on out-of-phase image compared with in-phase (f). (h) Sagittal contrast-enhanced T1-weighted fat-suppressed MR image shows corresponding avid enhancement.

on gad-enhanced fat-suppressed T1sequence in 31 out of 32 patients. One false-negative study with no appreciable signal alteration or contrast enhancement on group B sequences was encountered, but leukemic infiltration was later seen on one month follow up MRI study and confirmed with biopsy results.

On the other hand unenhanced-mp MRI sequences (group A) qualitatively and quantitatively correctly diagnosed 30 out of 32 patients with proved malignant lesions. They exhibited marked diffusion restriction on *b*-value 800 DWI, ADC mean value 0.623×10^{-3} mm^2/s $\pm$ 0.121×10^{-3} mm^2 SD and did not show signal dropout on opposed phase sequences (Figs. 4 and

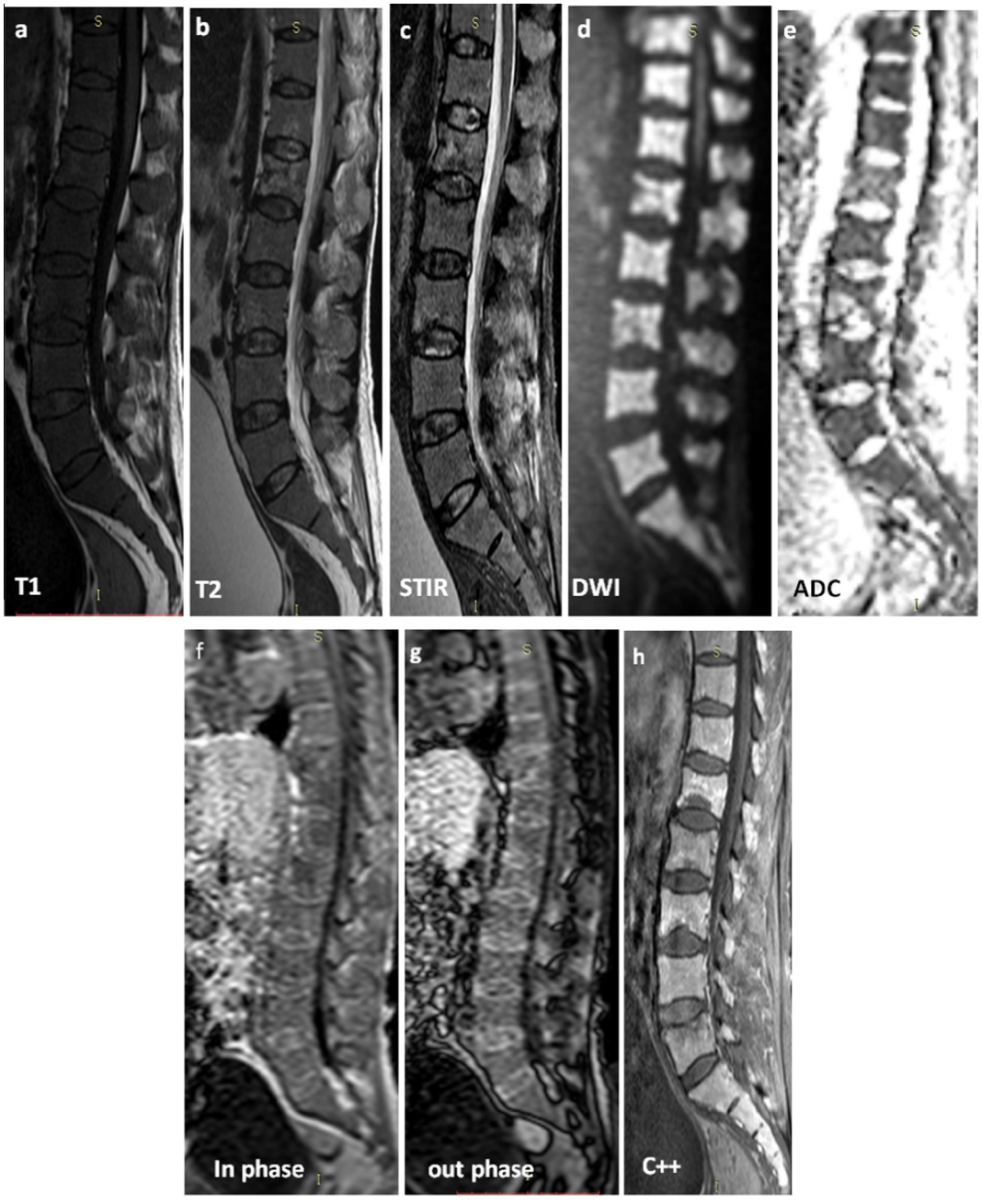

Fig. 4 A 58-year-old man with known lymphoma of the spleen presented with generalized bony aches. Unenhanced-mp MRI and gadolinium-enhanced MRI revealed diffuse marrow infiltration. (a) Sagittal precontrast T1-weighted spin-echo image shows diffuse low signal intensity of lumbosacral vertebrae isointense to muscle and intervertebral discs, consistent with bone marrow involvement. (b) Sagittal T2-weighted spin-echo image shows diffuse slightly high signal intensity of lumbosacral vertebrae and mild compression collapse with heterogenous signal of L1 vertebral body. (c) Sagittal STIR shows mild diffuse high signal intensity of lumbosacral vertebrae. (d) DWimage at *b*-value 800 s/mm^2 shows diffuse hyperintense signal of lumbosacral vertebrae. (e) ADC map shows an average apparent diffusion coefficient (ADC) value of 0.523×10^{-3} mm^2/s. (f) In-phase and (g) out-of-phase gradient-echo MR images show vertebral marrow appears slightly brighter on out-of-phase image compared with in-phase (f). (h) Sagittal contrast-enhanced T1-weighted fat-suppressed MR image shows diffuse bone marrow avid enhancement.

5). 2 out of 32 patients with malignant lesions were false negative, one had diffuse tiny lymphomatous infiltrates on top of hematopoietic marrow and the other patient had initial normal study, but the vertebral marrow infiltrations in both patients were later obvious on the 1 month follow up MRI and histopathological verification confirmed the diagnosis.

The ADC values recorded from the automatically created ADC maps differed significantly ($p < 0.001$) between

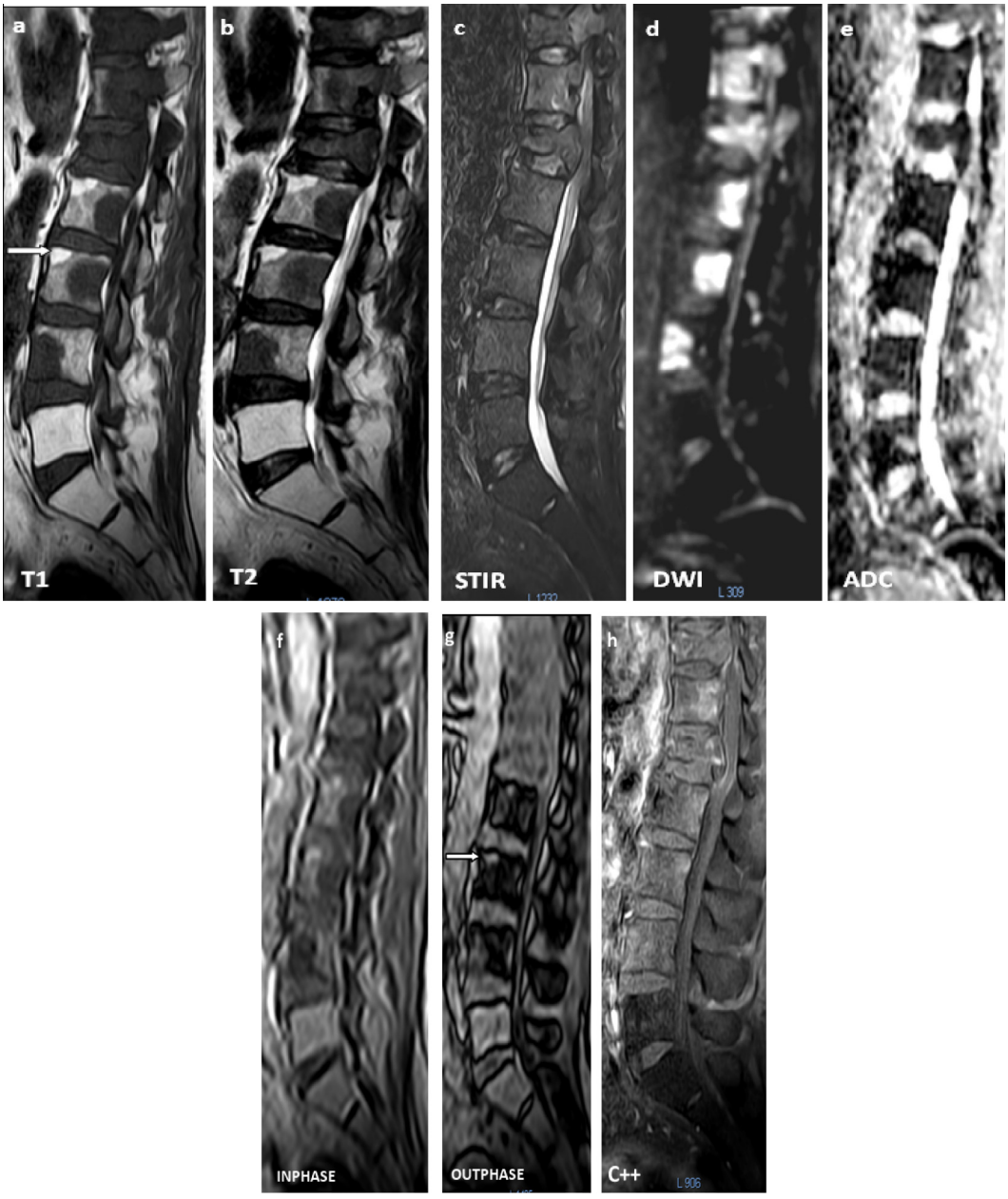

Fig. 5 A 75-year-old man with known prostate cancer received targeted radiotherapy for the prostate. The patient presented with generalized bony aches and bilateral sciatica. Unenhanced-mp MRI and gadolinium-enhanced MRI revealed focal and infiltrative marrow deposits. (a) Sagittal precontrast T1-weighted spin-echo image and (b) Sagittal T2-weighted spin-echo image shows focal low signal intensity marrow deposits involving D12, L2, L3 and L4 vertebrae as well as diffuse infiltration of D11 and L1 vertebrae. Compression collapse of L1 with retropulsion and thecal sac compression is noted. L5 and sacral vertebral bodies show fat marrow replacement due to radiation therapy targeting the prostate. (c) Sagittal STIR shows mild high signal intensity of the marrow lesions. (d) DW image at *b*-value 800 s/mm^2 shows focal and diffuse hyperintense signal corresponding to the low signal intensity lesions on T1WI. (e) ADC map shows average apparent diffusion coefficient (ADC) value of 0.624×10^{-3} mm^2/s. (f) in-phase and (g) out-of-phase gradient-echo MR images show vertebral marrow lesions appear brighter on out-of-phase image compared with in-phase (f). The fatty infiltrated L5 and sacral vertebrae remain hyperintense on both in- and out-of-phase images. Note that Modic type 2 degenerative marrow changes at L2 and L3 vertebral end plates have similar signal intensity as subcutaneous fat and do not dropout on out-of-phase imaging (*arrow*). (h) Sagittal contrast-enhanced T1-weighted fat-suppressed MR image shows a mild enhancement of the focal and infiltrative marrow lesions.

Table 1 Mean apparent diffusion coefficient values for normal, benign and malignant marrow lesions.

ADC value at *b*-800	Benign marrow lesion	Malignant marrow lesion	Normal marrow
Mean ADC values ± S.D*	Osteoporosis (0.189 ± 0.029) Red marrow (0.575 ± 0.212) Inflammatory/infective (1.641 ± 0.322)	0.506 ± 0.101	0.278 ± 0.083

* Data are mean ($\times 10^{-3}$ mm^2/s) ± standard deviation, ADC = apparent diffusion coefficient.

malignant (mean, 0.623×10^{-3} mm^2/s; SD ± 0.121×10^{-3} mm^2/s) and the following benign marrow entities, namely normal marrow (mean, 0.278×10^{-3} mm^2/s; SD ± 0.083×10^{-3} mm^2/s), osteoporosis (mean, 0.189×10^{-3} mm^2/s; SD ± 0.029×10^{-3} mm^2/s and infective /inflammatory marrow lesions (mean, $1.641 \pm 0.322 \times 10^{-3}$ mm^2/s; SD ± 0.322×10^{-3} mm^2/s). On the other hand the ADC values of malignant lesions and benign red marrow (mean, 0.575×10^{-3} mm^2/s; SD ± 0.212×10^{-3} mm^2/s) did not differ significantly with p value > 0.05 (Table 1 and Fig. 6).

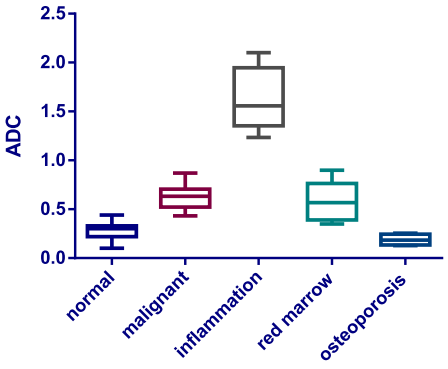

Fig. 6 Box plot showing differences in apparent diffusion coefficient (ADC) between normal, malignant, inflammation/infection, red marrow and osteoporosis. The line within the box marks median value.

Based on the above mentioned results of qualitative, quantitative image analysis and gold standard, the sensitivity, specificity, PPV, NPV and accuracy for differentiating benign from malignant vertebral marrow lesions on unenhanced-mp MRI and gadolinium-enhanced images added to conventional MRI are shown in Table 2. The sensitivity, specificity, and accuracy of unenhanced-mp MR images were 94%, 92%, and 93% and the T1-weighted fat-suppressed contrast-enhanced images added to conventional MRI were 97%, 88%, and 93%. There was no statistically significant difference between unenhanced-mp MRI and gadolinium-enhanced MRI (p value > 0.05) as regards their diagnostic performance in differentiating benign from malignant vertebral marrow infiltrative lesions.

We also calculated the scan duration of group (A) and group (B) included sequences (shown in Table 3) which was 15 min 22 s and 13 min 24 s respectively.

4. Discussion

In recent years, MRI has increasingly become the modality of choice for imaging musculoskeletal disorders (19–21). MRI is very sensitive to detect bone marrow metastases, although improving specificity needs a good understanding of normal and abnormal marrow appearance and a clever use of acquisition sequences and contrast media (22). The red marrow is more cellular and more perfused than the yellow marrow and contains only 40% fat compared to 80% fat in yellow

Table 2 The results of group (A) unenhanced-multiparametric MRI and group (B) conventional and gadolinium (Gad)-enhanced MRI studies.

	Total no of cases	TP	TN	FP	FN	Sensitivity (%)	Specificity (%)	PPV (%)	NPV (%)	Accuracy (%)
Group (A) unenhanced mp MRI	56	30	22	2	2	94	92	94	92	93
Group (B) conventional and Gad-enhanced MRI	56	31	21	3	1	97	88	91	95	93

TP true positive, TN true negative, FP false positive, FN false negative.

Table 3 Scan duration of unenhanced-multiparametric MRI study of group (A) and conventional/gadolinium-enhanced study of group (B).

Study group	Group (A)		Group (B)	
	Unenhanced mp MRI		Conventional and Gad-enhanced MRI	
Scan duration in minutes	Conventional	8:45	Conventional	8:45
	DWI	6:09	T1WI post contrast axial and sagittal	4:09
	IN/OUT phase	0:28	Time for contrast injection	0:30
Total scan duration in minutes		15:22		13:24

marrow (23,24). An often encountered diagnostic dilemma in the MRI interpretation is the difficulty in differentiating diffuse marrow infiltrative lesions from the highly variable appearance of normal hypercellular hematopoietic red marrow. The hypercellular red marrow may appear homogeneously diffuse, simulating a marrow-infiltrative tumor, or focal and patchy, simulating metastases (25). Skeletal muscles adjacent to bone or non-degenerated intervertebral disk are accurate internal standards and can serve as simple tools to help in differentiating normal and abnormal bone marrow on T1-weighted spin-echo MRI (18). In this study T1-weighted MRI accurately depicted and characterized the malignant multifocal metastatic deposits as well as focal and diffuse red marrow that exhibited signal intensity higher than adjacent muscle, but in 4 patients with profound red marrow reconversion and 4 patients with advanced osteoporosis (Fig. 2) or extensive bone marrow edema (Fig. 3), it was difficult to differentiate from malignancy based on T1-weighted image alone. Griffith et al. (26) reported that on T1-weighted images, osteoporosis can have a heterogeneous appearance because of decreased cellular marrow components and increased fat content. Also, hematopoietic marrow hyperplasia, diffuse inflammatory/infective marrow edema and diffuse malignant marrow infiltration showed diffuse high signal intensity on STIR sequence. Standard conventional MRI sequences were not specific for the characterization of infiltrative marrow lesions as 8 out of 56 cases were misinterpreted. This was in agreement with Beltran et al. (5) and Zhao et al. (18) who confirmed the non specificity of conventional imaging techniques.

Schmid et al. (27) concluded that addition of T1-weighted contrast-enhanced MR imaging does not alter the diagnosis of bone marrow abnormalities, and for most cases, they recommend performing only the STIR sequence. This was contradictory to our study supported by previous results of Rahmouni et al. (28), which revealed that the addition of gadolinium-enhanced T1 weighted sequence improved lesion conspicuity and characterization of our cases, although we agree with Daldrup-Link et al. (29), who reported that gadolinium-enhancement of the markedly hypercellular marrow and infiltrated marrow in patients with hematologic malignancies shows considerable overlap and is of limited clinical value for a definitive differentiation of these entities. This was in compliance with two false positive patients who had appreciable post-gadolinium bone marrow enhancement due to profound hypercellular hematopoietic red marrow. On the other hand one patient with early leukemic infiltrates was false negative on gadolinium-enhanced study, this was in agreement with Vande Berg et al. (16) who found normal bone marrow appearance and enhancement in early diffuse invasion by hematological malignancies. Mosher (13) reported that in clinical practice when faced with diagnostic uncertainty in the evaluation of abnormal marrow findings, indiscriminant use of contrast-enhanced images simply serves to confirm the obvious, with little diagnostic effectiveness. On the other hand the risks associated with administration of intravenous gadolinium based contrast medium, most notably, nephrogenic systemic fibrosis (30–32) can occur in patients with severe renal impairment, although it is rare in patients with normal renal function (33). Therefore, in this study, patients with severe renal impairment were excluded. Accordingly, we applied the two newly developed noncontrast-based DWI and opposed phase chemical shift MR techniques.

DWI should be considered a powerful functional technique for musculoskeletal imaging. The option of contrast-free scanning certainly is of clinical significance (34,35). The principle underlying DWI is based on the measurement of the restrictions on the Brownian motion of water molecules (36). Water movement is relatively impeded in tightly packed tumoral cells and high cellularity tissues appear persistently bright on low and high *b*-value DWI (37).

In this study we found that visual assessment of high signal intensity on high *b*-value (800) was not specific for malignancy because inflammation and hyperactive hematopoietic marrow can result in a similar diffusion restriction (Figs. 1 and 3),this was in agreement with Koh et al. (38) and Ballon et al. (39). On the other hand the quantitative assessment by measuring the ADC value was able to distinguish benign from malignant high signal intensity on DWI (Figs. 3 and 5).This was in agreement with Padhani et al. (14), who highlighted the necessity of correlating high *b*-value DW images with corresponding ADC values to prevent misinterpretation due to T2 shine-through. Our observations supported by other studies (14,40–43) showed that normal yellow marrow had the lowest ADC value and the infiltrated neoplastic marrow as well as hypercellular red marrow had higher ADC value, on the other hand the infective/inflammatory bone marrow lesion had the highest ADC value (Table 1 and Fig. 6). Thus, it was concluded that signal intensity and ADC value difference between yellow marrow and malignant marrow were not overlapping, but the signal intensity difference between malignant and inflammatory/infective lesion was overlapping although the ADC value difference between the two entities was statistically significant with p value < 0.001. On the other hand, in agreement with Padhani et al. (14), there was narrow signal intensity and ADC value difference between malignant and red marrow. In this study the narrow signal intensity difference hindered the depiction of minor marrow infiltration on top of hyperactive red marrow in 2 patients.

In this study the diagnostic problem of narrow signal intensity difference between hypercellular red marrow and malignant infiltration was almost solved by the addition of in/out-of-phase chemical shift sequence to the unenhanced-mp MRI protocol. Chemical shift imaging takes advantage of the small differences in precession frequency between fat and water protons to determine the presence of microscopic fat and water within the same imaging voxel. If a given voxel contains both fat and water, drop of signal on out-of-phase images will be noted (44).

On the other hand, lesions composed of virtually 100% fat will not show a drop of signal on out-of-phase sequence (11), this was in concordance with our findings where hemangioma, fat island, Modic type 2 vertebral endplate marrow changes and radiotherapy induced profound fatty marrow did not exhibit signal dropout (Fig. 5).

Red marrow shows normal signal dropout on out-of-phase images because of the presence of both fat and water cells, on the other hand most neoplasms completely replace or displace fat in the marrow space; thus, the neoplastic area will lack normal signal dropout on out-of-phase images (45–47) and this was consistent with our findings (Figs. 1 and 4) .

Roberts et al. (1) suggested out-of-phase sequence to best assess for marrow replacement by tumor. In this study 7 out of 9 cases with hypercellular red marrow showed a drop in signal intensity on out-of-phase images (Fig. 1), but no drop in

signal intensity was noted in malignant marrow lesions (Figs. 4 and 5), these results were concordant with Moulopoulos et al. (48). However, 2 of 9 cases with hypercellular red marrow did not exhibit visually obvious signal dropout on opposed phase images, this was likely attributed to extremely hypercellular marrow after bone marrow transplantation, that vigorously replaced the fat cells.

In this unenhanced-mp MRI (group A) study the addition of chemical shift sequence improved the MRI diagnostic performance in discriminating between benign and malignant marrow lesions.

Our results showed that the sensitivity, specificity and accuracy for unenhanced-mp MRI (group A) were 94%, 92%, and 93% respectively, which were almost comparable to those calculated for gadolinium-enhanced MRI (group B), where sensitivity of 97%, specificity of 88% and accuracy of 93% were reported. While the overall diagnostic performance of gadolinium-enhanced MRI and unenhanced-mp MRI may be similar, the latter has the advantage of not using intravenous contrast media.

The scan duration of unenhanced-mp MRI (group A) was 2 min longer than gadolinium-enhanced (group B) study.

To our knowledge, the diagnostic value of unenhanced-mp MRI in comparison with gadolinium-enhanced imaging in the evaluation of marrow infiltrative lesions has not been reported. Further investigation is recommended to establish the unenhanced mp MRI as a reliable alternative technique to contrast based MRI in clinical practice and its impact on monitoring treatment response, however this latter issue was beyond the scope of this study.

In conclusion, according to the results of this study, unenhanced-multiparametric MRI is compatible with gadolinium-enhanced MRI in reliable characterization of marrow infiltrative lesions. The routine MRI protocol of cancer patients should be altered to accommodate the evolving MRI technology and cost effectively substitute the need for gadolinium enhanced scan.

Conflict of interest

We have no conflict of interest to declare.

Acknowledgement

We express sincere appreciation to Ahmed ElSayed AbdelAziz, the MRI technician, for his invaluable work in performing the examinations.

References

(1) Roberts C, Daffner R, Weissman B, et al. ACR appropriateness criteria on metastatic bone disease. J Am Coll Radiol 2010; 7:400–9.
(2) Schaffer DL, Pendergrass HP. Comparison of enzyme, clinical, radiographic, and radionuclide methods of detecting bone metastases from carcinoma of the prostate. Radiology 1976;121: 431–4.
(3) Hanrahan C, Shah L. MRI of spinal bone marrow: part 2, T1-weighted imaging-based differential diagnosis. AJR 2011;197:1309–21.
(4) Hanna SL, Fletcher BD, Fairclough DL, et al. Magnetic resonance imaging of disseminated bone marrow disease in patients treated for malignancy. Skeletal Radiol 1991;20:79.
(5) Beltran J, Shankman S. MR imaging of bone lesions of the ankle and foot. Magn Reson Imaging Clin N Am 2001;9:553–66.
(6) Baur A, Reiser MF. Diffusion-weighted imaging of the musculoskeletal system in humans. Skeletal Radiol 2000;29(10): 555–62.
(7) Kim HK, Wang LL, Merrow AC, et al. Compounding factors affecting fat and water content of skeletal muscles in healthy children; objective measures using T2 relaxation time mapping (T2 Map). Chicago: Radiological society of North America; 2011.
(8) Zaraiskaya T, Kumbhare D, Noseworthy MD. Diffusion tensor imaging in evaluation of human skeletal muscle injury. J Magn Reson Imaging 2006;24(2):402–8.
(9) Sinha S, Sinha U, Edgerton VR. In vivo diffusion tensor imaging of the human calf muscle. J Magn Reson Imaging 2006;24(1): 182–90.
(10) Rosen BR, Fleming DM, Kushner DC, et al. Hematologic bone marrow disorders: quantitative chemical shift MR imaging. Radiology 1988;169:799–804.
(11) Zajick Jr DC, Morrison WB, Schweitzer ME, Parellada JA, Carrino JA. Benign and malignant processes: normal values and differentiation with chemical shift MR imaging in vertebral marrow. Radiology 2005;237:590–6.
(12) Harned EM, Mitchell DG, Burk Jr DL, Vinitski S, Rifkin MD. Bone marrow findings on magnetic resonance images of the knee: accentuation by fat suppression. Magn Reson Imaging 1990;8: 27–31.
(13) Mosher T. Diagnostic effectiveness of gadolinium-enhanced MR imaging in evaluation of abnormal bone marrow signal. Radiology 2002;224:320–2.
(14) Padhani A, van Ree K, Collin D, et al. Assessing the relation between bone marrow signal intensity and apparent diffusion coefficient in diffusion-weighted MRI. AJR 2013;200:163–70.
(15) Moulopoulos LA, Varma DGK, Dimopoulos MA, et al. Multiple myeloma: spinal MR imaging in patients with untreated newly diagnosed disease. Radiology 1992;185:833–40.
(16) Vande Berg BC, Lecouvet FE, Michaux L, Ferrant A, Maldague B, Malghem J. Magnetic resonance imaging of the bone marrow in hematological malignancies. Eur Radiol 1998;87:1335–44.
(17) Swartz PG, Roberts CC. Radiological reasoning: bone marrow changes on MRI. AJR 2009; 193(Suppl.):S1–S4.
(18) Zhao J, Krug R, Xu D. et al. MRI of the Spine: image quality and normal-neoplastic bone marrow contrast at 3 T versus 1.5 T. AJR 2009;192:873–880.
(19) Guermazi A, Roemer FW, Hayashi D. Imaging of osteoarthritis: update from a radiological perspective. Curr Opin Rheumatol 2011;23:484–91.
(20) Farrant JM, O'Connor PJ, Grainger AJ. Advanced imaging in rheumatoid arthritis. Part 1: synovitis. Skeletal Radiol 2007;36: 269–79.
(21) Khoo MMY, Tyler PA, Saifuddin A, Padhani AR. Diffusion-weighted imaging (DWI) in musculoskeletal MRI: a critical review. Skeletal Radiol 2011;40:665–81.
(22) Vanel D. MRI of bone metastases: the choice of the sequence. Cancer Imaging 2004;4(1):30–5.
(23) Vogler JB, Murphy WA. Bone marrow imaging. Radiology 1988;168:679–93.
(24) Chen WT, Shih TT, Chen RC, et al. Vertebral bone marrow perfusion evaluated with dynamic contrast-enhanced MR imaging: significance of aging and sex. Radiology 2001;220:213–8.
(25) Hartman RP, Sundaram M, Okuno SH, Sim FH. Effect of granulocyte-stimulating factors on marrow of adult patients with musculoskeletal malignancies: incidence and MR findings. AJR Am J Roentgenol 2004;183:645–53.
(26) Griffith JF, Yeung DK, Antonio GE, et al. Vertebral bone mineral density, marrow perfusion, and fat content in healthy men and men with osteoporosis: dynamic contrast-enhanced MR imaging and MR spectroscopy. Radiology 2005;236:945–51.

(27) Schmid MR, Hodler J, Vienne P, Binkert CA, Zanetti M. Bone marrow abnormalities of foot and ankle: STIR imaging versus T1-weighted contrast-enhanced fat-saturated spin-echo MR imaging. Radiology 2002;224:463–9.
(28) Rahmouni A, Montazel J, Divine M, et al. Bone marrow with diffuse tumor infiltration in patients with lymphoproliferative diseases: dynamic gadolinium enhanced MR imaging. Radiology 2003;229:710–7.
(29) Daldrup-Link H, Henning T, Link TMR imaging of therapy-induced changes of bone marrow. Eur Radiol 2007;17:743–761.
(30) Tehranzadeh J, Ashikyan O, Dascalos J. Advanced imaging of early rheumatoid arthritis. Radiol Clin N Am 2004;42:89–107.
(31) Shabana W, Cohan R, Ellis J, Hussain H, Francis I, et al. Nephrogenic systemic fibrosis: a report of 29 cases. AJR Am. J Roentgenol 2008;190:736–41.
(32) Marckmann P, Skov L, Rossen K, Dupont A, Damholt MB, et al. Nephrogenic systemic fibrosis: suspected causative role of gadodiamide used for contrast-enhanced magnetic resonance imaging. J Am Soc Nephrol 2006;17:2359–62.
(33) Ostergaard M, Conaghan PG, O'Connor P, Szkudlarek M, Klarlund M, Emery P, et al. Reducing invasiveness, duration, and cost of magnetic resonance imaging in rheumatoid arthritis by omitting intravenous contrast injection—does it change the assessment of inflammatory and destructive joint changes by the OMERACT RAMRIS? J Rheumatol 2009;36:1806–10.
(34) Neubauer H, Platzer I, Mueller V, Meyer T, Liese J, Koestler H, et al. Diffusion-weighted MRI of abscess formations in children and young adults. World J Pediatr 2012;8:229–34.
(35) Goo HW. Regional and whole-body imaging in pediatric oncology. Pediatr Radiol 2011;41:S186–94.
(36) Borrero CG, Mountz JM, Mountz JD. Emerging MRI methods in rheumatoid arthritis. Rheumatology 2011;7:85–95.
(37) Padhani A, Koh DM, Collins D. Whole-body diffusion-weighted mr imaging in cancer: current status and research directions. Radiology 2011;261:3.
(38) Koh D, Blackledge M, Padhani A, et al. Whole-body diffusion-weighted MRI: tips, tricks, and pitfalls. AJR 2012;199:252–62.
(39) Ballon D, Watts R, Dyke JP, et al. Imaging therapeutic response in human bone marrow using rapid whole-body MRI. Magn Reson Med 2004;52:1234–8.
(40) Messiou C, Collins DJ, Morgan VA, Desouza NM. Optimising diffusion weighted MRI for imaging metastatic and myeloma bone disease and assessing reproducibility. Eur Radiol 2011;21(8):1713–8.
(41) Hillengass J, Bäuerle T, Bartl R, et al. Diffusion-weighted imaging for non-invasive and quantitative monitoring of bone marrow infiltration in patients with monoclonal plasma cell disease: a comparative study with histology. Br J Haematol 2011;153(6):721–8.
(42) Chan JH, Peh WC, Tsui EY, et al. Acute vertebral body compression fractures: discrimination between benign and malignant causes using apparent diffusion coefficients. Br J Radiol 2002;75(891):207–14.
(43) Chen WT, Shih TT, Chen RC, et al. Vertebral bone marrow perfusion evaluated with dynamic contrast-enhanced MR imaging: significance of aging and sex. Radiology 2001;220(1):213–8.
(44) Gokalp G, Mutlu FS, Yazici Z, Yildrim N. Evaluation of vertebral bone marrow fat content by chemical-shift MRI in osteoporosis. Skeletal Radiol 2011;40:577–85.
(45) Seiderer M, Staebler A, Wagner H. MRI of bone marrow: opposed-phase gradient-echo sequences with long repetition time. Eur Radiol 1999;9:652–61.
(46) Zampa V, Cosottini M, Michelassi C, Ortori S, Bruschini L, Bartolozzi C. Value of opposed-phase gradient-echo technique in distinguishing between benign and malignant vertebral lesions. Eur Radiol 2002;12:1811–8.
(47) Eito K, Waka S, Naoko N, Makoto A, Atsuko H. Vertebral neoplastic compression fractures: assessment by dual-phase chemical shift imaging. J Magn Reson Imaging 2004;20:1020–4.
(48) Moulopoulos LA. Effect of treatment on normal tissue: bone marrow. In: Husband JE, Reznek RH, editors. Imaging in oncology. London: Taylor & Francis; 2004, p. 1277–1287.